This article has been accepted for publication in a future issue of this journal, but has not been fully edited. Content may change prior to final publication. Citation information: DOI 10.1109/RBME.2017.2706966, IEEE Reviews in Biomedical Engineering

Haptic Feedback in Needle Insertion Modeling and Simulation: Review

Gourishetti Ravali, Muniyandi Manivannan*

***Abstract*—Needle insertion being the most basic skill in medical care, training has to be imparted not only for physicians but also for nurses and paramedics. In most needle insertion procedures haptic feedback from the needle is the main stimulus that novices are to be trained in. For better patient safety, the classical methods of training the haptic skills have to be replaced with simulators based on new robotic and graphics technologies. This paper reviews the current advances in needle insertion modeling. It is classified into three sections: needle insertion models, tissue deformation models, and needle-tissue interaction models. Although understated in the literature, the classical and dynamic friction models which are critical for needle insertion modeling are also discussed. The experimental set-up or the needle simulators which have been developed to validate the models are described. The need of psychophysics for needle simulators and psychophysical parameter analysis of human perception in needle insertion are discussed, which are completely ignored in the literature.**

***Index Terms*—haptic feedback; minimally invasive procedure; needle insertion procedures; needle insertion modeling; psychophysics**

I. Introduction

MINIMALLY invasive procedures have become important medical techniques in many modern clinical practices due to their advantage of having small incisions compared to traditional surgical procedures with large openings. Needle insertion procedure is a vital element in most minimally invasive procedures [1]. The various applications of needle insertion in minimally invasive procedures would include needle biopsies [2], [3]; regional anesthesia [4], [5]; injections [6]; angiography [7]; laparoscopy which requires veress needle insertion [8], [9]; endoscopy [10]; brachytherapy cancer treatment [11]–[13]; spine and neurosurgery [14], [15]. Therefore, training the novice with needle insertion plays a major role in the current practice of healthcare. Needle insertion is one of the basic skills in medical care that all clinicians have to be trained in to have good efficiency and high accuracy. During the training process of clinicians, long period of time is allocated for developing psychomotor skills such as needle insertion and establishing an intravenous drip [16]. It is considered that the success rate is directly proportional to the skills and the experience of the physician or clinician [17].

Needle insertion procedures involve three basic steps where physicians can make mistakes: determination of the insertion point, needle orientation, and needle movement into soft tissues. Besides these, the physician may get deflected from the target because of tissue deformation [18] and motion artifacts of the patient. The needle's path may traverse some sensitive tissues such as nerves, bones, arteries, or organs. Adverse damage to these tissues may lead to many side effects. Therefore, it is important that the needle does not cause any damage to these crucial tissues [19]. Other causes of inaccuracy in needle procedures are due to the differences in tissue type involved in each procedure, physiological changes in the organ between the planning and treatment phases, differences in mechanical properties of healthy and diseased tissue or dead tissue (cadavers), and the variability in the properties of soft tissue for different patients [20].

A. Problems in needle insertion training

Traditionally, physicians are trained with cadavers, porcine, or bovine samples and then with anesthetized animals. However, the material properties of the tissues would vary between cadavers and live patients [20]. Thus, these traditional techniques may lead to several inaccuracies with live patients, resulting in a lack of representative materials for accurate training. The current method of training novice for needle procedures in medical schools is by apprenticeship method in which the patient's safety is at risk [21]. Even traditionally trained doctors who performed needle procedures have shown high failure rates as shown in a recent survey [22]. This survey was performed at the University of Washington Medical Center on Acute Pain and they found a failure rate of 32% for thoracic needle procedures and 27% for lumbar epidural anesthesia procedures. They have also classified the causes of these failures (their failure rates) into five categories as dislodged catheter (17%), not in epidural space (11%), one-sided block (7%), develop a leak (7%), uncertain cause (58%). With increased focus on patient safety, new technological training solutions are essential for reducing errors during the needle procedures.

B. Medical simulation as a technological solution

Medical simulation is one of the widely used technologies in clinical education with the goal of training the novice in medical skills and improving the learners' efficiency and confidence in the corresponding tasks. Medical simulators have multiple benefits over traditional training methods such as patients' safety, physicians get to trained in different scenarios by changing the properties of the tissues in an administered environment that make them familiar with both common and rare cases [23], and flexible training opportunities as trainees do not require a direct supervision of trained clinicians [24],

M.Manivannan* is with Haptics Lab, Biomedical Engineering Group, Applied Mechanics Department, Indian Institute of Technology Madras, Chennai-600036. (corresponding author email id: mani@iitm.ac.in).

This article has been accepted for publication in a future issue of this journal, but has not been fully edited. Content may change prior to final publication. Citation information: DOI 10.1109/RBME.2017.2706966, IEEE Reviews in Biomedical Engineering

The major advantage of medical simulators is the quantification of performance during the training session which will help the trainees with steeper learning curves, eventually reducing their failure rates [25]. Since accurate force feedback is the key factor in needle simulators, it is necessary that the simulators provide better haptic feedback to train the physicians [17].

C. Haptic Feedback in Medical Simulators

Many medical procedures often involve the use of the force feedback to manipulate organs or tissues by using special tools [26]. Some of the medical procedures such as palpation, surgical interventions, phlebotomy and other interventional procedures are examples where the force feedback is of great importance [27]. In minimally invasive procedures, the force feedback has reduced compared to open surgery where the clinicians rely more on the feeling of net forces resulting from tool-tissue interactions and thereby there is a high requirement for training to have a successful surgery. The training for minimally invasive procedures depends on the education and improvement of the trainee's haptic sensorimotor system [28]. In order to enhance the training applications, medical simulators are equipped with haptic feedback [29]. The need of haptic feedback starts with the basic physical examination technique, palpation which is a supplementary interaction technique to diagnose a disease or illness [30]. Therefore, the haptic feedback is the basic parameter for the palpation simulators.

During the needle insertion procedures, doctors rely on both visual and haptic feedback. The visual feedback (to determine the position of the needle tip) is acquired from the segment of the needle remaining outside the body. Physicians also rely on their mental 3D visualization of the anatomical structures [31]. Haptic feedback has great significance as the insertion forces vary depending on the depth of penetration and the type of tissue through which the needle penetrates. The detection of changes in tissue properties at different depths during needle insertion is important for needle localization and detection of subsurface structures. However, changes in tissue mechanical properties deep inside the tissue are difficult for the novice to sense because the relatively large friction force between the needle shaft and the surrounding tissue masks the smaller tip forces [32]. This method of predicting the location of a needle inside the body is possible only with *in vivo* experience, which is a great challenge for the novice and therefore, the need of training with force feedback is substantially increased and thereby the haptic feedback is included as a key parameter during the development of needle simulators.

D. Survey Method

The survey includes papers that discussed needle deflection models, tissue deformation models, needle-tissue interaction force models, friction models, details of experiments related to needle insertion and also few papers related to need of psychophysics for medical simulators. The papers for the review were chosen from Google Scholar, the Scitopia.org search engine, and the Medline/PubMed database. The sections in the review have been organized based on the topics mentioned above.

E. Scope of this Review

This paper reviews the current state-of-the-art needle insertion simulations. It also elaborates the need for frictional models which are neglected in the literature and introduces the need for psychophysics in the design of needle insertion simulators towards the improvement in accuracy.

II. Overview of needle insertion modeling

The needle insertion simulation procedures would include three major modeling stages as shown in Fig. 1: modeling of needle deflection, modeling of tissue deformation, and modeling of needle-tissue interaction forces. The various techniques available for modeling these three phases are:

- Finite Element Methods (FEM) based models.
- Beam based models.
- Mass Damper models (mass is neglected).

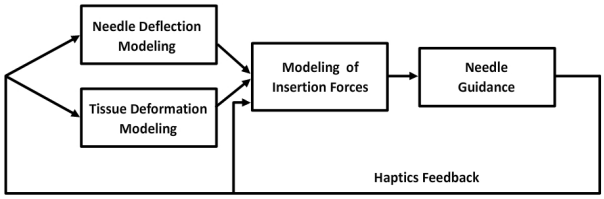

Fig. 1: Schematic of needle insertion simulation

Using Finite Element Modeling (FEM), the deformations of soft tissues with the force applied on the needle are computed for both static and dynamic behaviors of soft tissues by considering displacement, velocity, and acceleration at each nodal point [19], [33], [34].

In beam-based modeling, the needle insertion forces are computed. Apart from this, the bending and twisting of the needle inside the tissues which occur due to the reactive forces of the tissues are studied [35]–[37] as shown in Fig. 2.

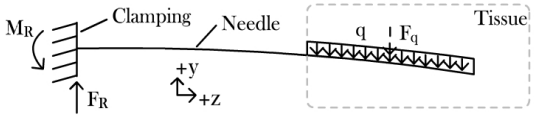

Fig. 2: The distributed tissue reaction force acting along the needle shaft to the portion of the needle that is inserted into the tissue. F_R is the reaction force at the needle base [37]

.

Spring-Damper models are mainly used for tissue deformation modeling where the deformation forces have been considered as pre-puncture and post-puncture forces [18], [38], [39].

Hing et al. [17] identified that quantification of the insertion forces was an important factor in developing a simulator which gives an accurate force measurement and provides an accurate input for modeling the needle-tissue interaction. A 6 Degree of Freedom (DOF) force sensor was used to measure the total interaction force, which is a summation of the cutting and frictional forces. The cutting force was measured to be the difference of the total interaction force and the frictional force.

This article has been accepted for publication in a future issue of this journal, but has not been fully edited. Content may change prior to final publication. Citation information: DOI 10.1109/RBME.2017.2706966, IEEE Reviews in Biomedical Engineering

The frictional force was measured during the withdrawal of the needle where no cutting of the tissues was involved.

Brett et al. [40] developed an experimental simulator with a 1 DOF force measuring arrangement. They studied the force variation corresponding to the depth of penetration for different velocities and found that the ligamentum flavum is the tissue which requires the highest amount of force (15 N) for its puncture. They also found the force required at the supraspinous ligament (around 15 N) and also muscle fibers (5 N). Naemura et al. [41] developed an epidural simulator similar to Brett's and validated their models using the literature data and they could find two peaks in the process of puncture. Their results prove that their simulator has forces very comparable to those of a conventional simulator.

Gerwen et al. [42] provide an overview of research related to the force measurement data obtained during needle insertion. They have clearly classified various papers into a set of four categories based on experimental data, statistical analysis, and sample size. They also studied the effect of needle characteristics, tissue characteristics and insertion method on axial forces. This data can be used for needle modeling, tissue modeling, and needle-tissue interaction modeling.

III. Modeling of Needle Insertion Forces

During the needle insertion procedures, needle orientation, needle bending, and tissue deformation are the three effects which lead to inaccurate positioning of the needle. Reaching the target location in a needle insertion procedures require high skill, training, and experience. Therefore, accurate models of needles are required to train a novice. The total reaction force during a needle insertion procedures involves forces such as cutting force, kinetic friction, static friction, compression force, and torque as shown in Fig. 3.

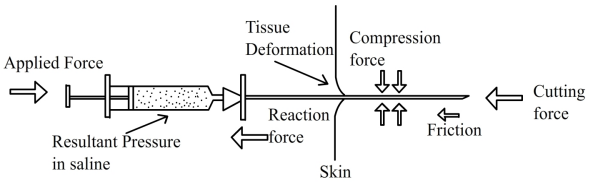

Fig. 3: Forces involved during needle insertion procedures [43]

.

A. Constraints of Needle Modeling

The main constraints for making an accurate model of insertion forces are the peak force during the insertion procedure, delay in the force changes (i.e. real-time detection of force changes), and identification of various parameters such as stiffness which is the cutting force on the tissue, friction during the sliding of the needle, and damping force [20]. Fig. 5 shows the schematic of needle insertion forces and also the indentation caused to the tissue during the needle insertion procedures.

B. Needle Models

The basic methods of needle modeling are as follows.

1) FEM using triangular elements: They consider the nonlinear inelastic behavior of needle forces as a function of displacement which leads to a set of nonlinear algebraic equations which are solved using numerical methods [44].
2) FEM using nonlinear beam elements: They consider the Euler-Bernoulli beam element which uses cubic and linear interpolation functions for the transverse and axial strain/displacement respectively. The equilibrium equation for the axial force, lateral force, and torque are solved using some iterative methods.
3) Angular spring model: The authors used this method to model a needle as a beam connected at one end, i.e. a cantilever beam. It is considered to have a number of rigid rods connected with springs which have rotational DOF. The nonlinear equations between the force and the joint angles by the rotational springs are solved by simple vector algebraic equations [45].

Goksel et al. [45] modeled a needle as a discrete structure composed of a finite number of rigid rods. The bending and twisting deformations in the needle structure would apply some internal reaction forces to restore its original configuration. To study the effect of these deformations on the overall insertion forces, these torques were modeled using two rotational springs, one for unbending and the other for untwisting the needle segment as shown in Fig. 4.

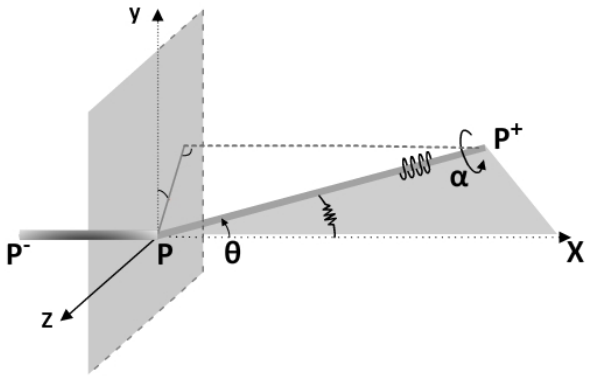

Fig. 4: Angles of bending and twisting between two needle segments [45]

.

Kataoka et al. [46] modeled a needle based on the Euler-Bernoulli beam theory that calculates the relationship between the beam deflection and the applied load. This model uses a distributed load along the needle shaft to evaluate the deflection of the needle tip. However, this resulted in an offset from the estimated needle tip deflection. Abolhassani et al. [20] also studied the needle model based on the Euler-Bernoulli beam theory as shown in Fig. 5.

Lehmann et al. [37] modeled a needle as a Euler-Bernoulli beam structure which is considered as a cantilever beam since it is fixed only at the base. They simulated the needle insertion forces based on the static deflection of the beam. These needle

This article has been accepted for publication in a future issue of this journal, but has not been fully edited. Content may change prior to final publication. Citation information: DOI 10.1109/RBME.2017.2706966, IEEE Reviews in Biomedical Engineering

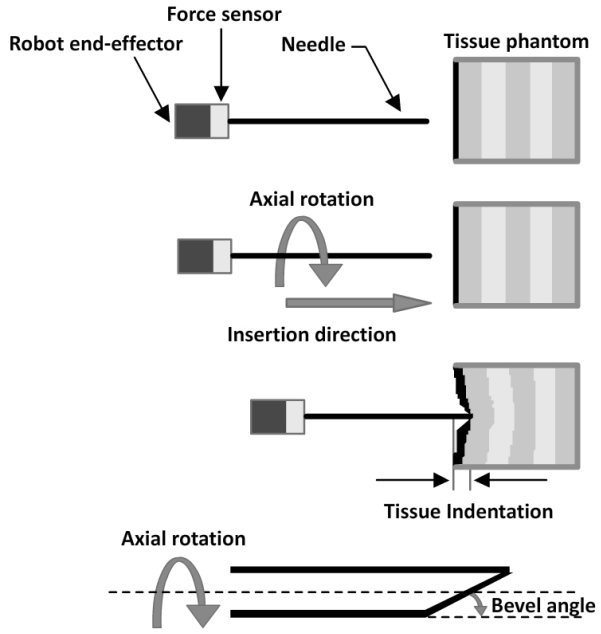

Fig. 5: Schematic indication of needle insertion forces and tissue deformation [20]

.

insertion forces on the beam and the beam deflection are given by the Euler-Bernoulli beam theory. They considered the location of the resultant force in the space as the area centroid of the distributed load. They formulated the force-displacement relation by considering the force applied on the needle base (F_R) as the summation of the load per unit length of the needle, which is given as

$$F_R = F_q = \int_{L-l_0}^{L} q(z)dz$$

where q represents the load gradient, l_0 represents the length section of needle outside the tissue and L represents the section of the needle inside the tissue.

Asadian et al. [44] modeled a needle as a beam-based model which comprises two connected beams, one beam at the section of the needle outside the tissue, and the other at the section of the needle inside the tissue. This representation gives the mental visualization of the location of the needle tip inside the tissues along with the typical haptic feedback from the simulators. Khadem et al. [47] extended the beam theory to develop a needle model with a novel approach by considering velocity as an input.

Okamura et al. [48] measured the needle insertion forces with the help of experimentation using a robotic assisted set-up during percutaneous insertion by separation of the total interaction forces as the cutting force and frictional force. The cutting force is caused due to the fracture of the tissue during needle insertion and, the frictional force is due to the sliding of the needle shaft through the tissues. They studied the needle bending effects and also the effect of insertion forces with various types of needles.

Misra et al. [49] considered tissue as a nonlinear hyperelastic material and modeled needle steering as an energy based formulation. This model has the advantage of deflections in 2 DOF, i.e. lateral and axial deflection of the needle. This model also studied the needle tip forces and the needle base forces that are applied by the trainee. However, the effects of frictional forces during needle insertion and the effects of needle insertion velocity were not considered.

Mahvash and Dupont [50] studied the effect of insertion velocity on tissue deformation and needle insertion force. They classified the needle insertion procedures into several events such as loading deformation, rupture, cutting, and unloading deformation events. They considered a nonlinear visco-elastic Kelvin model for the analysis of the relationship between rupture force and deformation of the tissue.

Farber et al. [51] modeled a virtual needle as a rod which provided the information on needle tip forces and needle body forces. The needle tip forces include the pre-puncture force, cutting force, and friction force. Needle body forces include the restriction forces by the transversal and rotational motion of the needle in soft tissues.

IV. Modeling of Tissue Deformation Forces

The study of tissue deformation forces and thereby of tissue modeling has great importance in the development of needle simulators. This study is mainly focused on the skin, vessels, muscles, brain, and heart tissues. Tissue modeling is always a challenge because of various tissue properties such as inhomogeneity, non-linearity, anisotropic layeredness, and visco-elasticity [52]. Among these various tissue properties, layeredness is very relevant to needle insertion. Each layer of the tissue is modeled differently based on the corresponding properties for particular applications. For example, in percutaneous therapies, when the needle punctures different tissues such as skin, muscle, adipose tissue, and some connecting tissues [53], each layer requires a different force to puncture it. The force not only varies for different layers but also varies for subjects based on their age, gender, body weight and so on [54].

A. Constraints of Tissue Modeling

For tissue modeling in any simulator, tissue deformation, and computation time complexity are the two main constraints. The accuracy of tissue deformation is the main criterion in training the novice in surgical procedures and computation time is the main criterion in surgical planning tasks [55].

In this paper, we consider the first criterion where training is the primary task. Therefore, the accuracy of tissue deformation is the primary constraint to be considered.

B. Tissue Models

The basic methods of tissue modeling are classified into three categories: phenomenological, structural, and structurally-based phenomenological models [56].

Phenomenological models consider tissue as a homogeneous material for determining the deformation mechanics,

This article has been accepted for publication in a future issue of this journal, but has not been fully edited. Content may change prior to final publication. Citation information: DOI 10.1109/RBME.2017.2706966, IEEE Reviews in Biomedical Engineering

neglecting the structural properties of the tissues. The mechanical properties of these models are written as a constitutive equation that relates stress and strain. Structural models consider tissue as a composite material: they are described by nonlinear algebraic equations between the stress and strain. The third category of the model which is a combination of the above two models can incorporate the particular structural arrangements and deformation mechanics.

DiMaio et al. [31] and Goksel et al. [57] modeled tissue using FEM with triangular elements. DiMaio considered tissue as homogeneous, linear, and elastostatic material that gives the deformations in two dimensions: axial, and transverse direction. The tissue deformation forces are formulated using the total strain energy E_{strain} phenomenon as a function of force and displacement, given by

$$E_{strain} = \frac{1}{2}\int_{\Omega} \epsilon^T(x)\sigma(x)dx$$

where Ω is the area of the solid body, σ is stress and ϵ is strain.

Lepiller et al. [58] modeled tissue using a novel FEM known as Eulerian hydrocode which was developed against large deformation problems such as plastic forming. Tissue deformation was achieved by a drift of neighbor elements like fluid according to both Euler equation and constitutive equations for solid.

Glozman and Shoham [36] presented the needle as a set of virtual springs. They modeled the tissue deformation forces as a function of needle penetration. The deeper the needle penetrates into the tissue, the greater is the number of springs, hence the forces are calculated considering the new set of springs at the tip, as shown in Fig. 6.

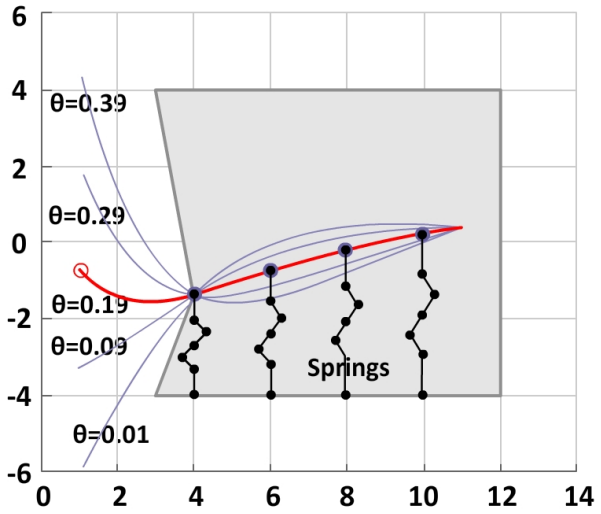

Fig. 6: Several needle path solutions for the same tip position with different tip inclinations [36]

Hing et al. [17] conducted an experiment to quantitatively measure the tissue deformation forces during needle insertion. These forces were used to model liver tissue in 3D FEM. Tissue deformation was modeled using the mesh locations.

Xu et al. [59] modeled both the tissue and the needle as a set of nodes and established the relation between external force and the tissue deformation by total potential energy. They considered the total potential energy as the difference between the strain energy of the tissue and work done by external forces. The tissue deformation is computed from the external forces and nodal displacements.

Barb et al. [60] proposed an algorithm to estimate forces in real time involved in needle insertion procedures. They approached the model based on Diolaiti et al. [61] who modeled soft tissues both as visco-elastic linear and nonlinear for estimation of real-time interaction forces of robots. Barb and Bayle used recursive parameter estimation algorithms for the real-time estimation of forces. They also considered the needle insertion procedures in different phases which were mentioned in the paper earlier: first, the needle pre-puncturing phase which gave the details of visco-elastic properties of the soft tissues; second, the puncturing phase which included the force required to puncture the tissues and also the effects of frictional force by the tissues on the shaft of the needle; and finally, the needle retraction phase which included the frictional force in the opposite direction of the puncturing phase. The soft tissues for stiffness measurement were modeled using two basic models, the Kelvin-Voigt model (KV model), and the Hunt-Crossley model (HC model).

Wang et al. [62] modeled frictional force with the consideration of relative velocity and contact length. The tissue is modeled using one of the basic models, the KV model. They considered the contact area along the length of the needle shaft by separating the lengths into small regions dl as shown in Fig. 7 and the total frictional force as the integral of the entire length of the needle as

$$F_{friction} = \int_{l_c(t)}^{0} 2\pi r R_f(v^*)dl$$

where the co-efficient of frictional force R_f is defined as

$$R_f(v^*) = \frac{F_{friction}}{2\pi r L_c}$$

where r is the radius of the needle, $l_c(t)$ is the length of the needle, L_c is the tissue thickness, and $F_{friction}$ is the frictional force with respect to relative velocity.

Models of specific tissues such as arteries, ligaments, and skin were also reported in the literature. Gasser Ogden Holzapfel (GOH) formulated the relationship between force and displacement that represents the orthotropic hyperelastic behavior of arterial tissues [63]. Weiss et al. [64] modeled the ligaments of the knee joint and formulated the transversely isotropic hyperelastic behavior of ligaments. They considered the strain energy function for force analysis. For soft tissues, Limbert and Middleton [65] developed an anisotropic strain energy function. Limbert [66] developed a novel invariant based multiscale constitutive framework to characterize soft tissues as transversely isotropic and with orthotropic elastic behavior. The mechanical formulations were customized to model skin [56].

This article has been accepted for publication in a future issue of this journal, but has not been fully edited. Content may change prior to final publication. Citation information: DOI 10.1109/RBME.2017.2706966, IEEE Reviews in Biomedical Engineering

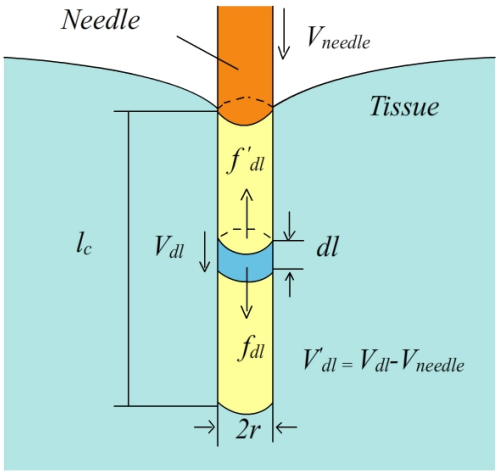

Fig. 7: Scheme of friction model during needle insertion procedures [62]

.

V. Modeling Needle-Tissue Interaction Forces

The study of needle-tissue interaction forces which are also known as total interaction forces includes both needle insertion and tissue deformation forces. The formulation of total interaction forces is the major challenge in developing a needle simulator.

With the complexities involved in needle-tissue interactions, it is not recommended to use a single combined mesh [67]. Therefore, needle-tissue interaction simulation involves two separate measures for tissue and needle modeling.

Golzman and Shoham [36] developed a robotic needle simulator for needle insertion and its movement control in soft tissues. They modeled interaction forces using a simplified virtual spring model where they considered a flexible needle as a linear cantilever beam supported by a series of virtual springs. They used forward kinematics which helps in computing the position of the end effector to enable needle insertion path planning and, inverse kinematics which helps in computing the joint parameters to enable path correction in real time.

For small displacements, Simone assumed the tissue force response on the needle shaft to be linear [39]. He modeled total interaction force as a summation of the lateral forces along the needle shaft in the virtual springs and frictional forces parallel to the needle axial direction.

Yan et al. [35] proposed a spring-beam damper system by considering tissue as nonlinear and elastic material as shown in Fig. 8. Their model formulates the system dynamics during force application on the needle end using Hamilton's principle. The flexible needle is assumed to follow the Bernoulli-Euler beam model.

Limitations of this model considered by Yan and Ng are:

1) The needle has only 2 DOF, one in the insertion direction and the other in the steering direction where as the third DOF during needle insertion is neglected.
2) Only lateral compression of the beam is possible and not the longitudinal compression.
3) An assumption of constant spring and damper coefficients.

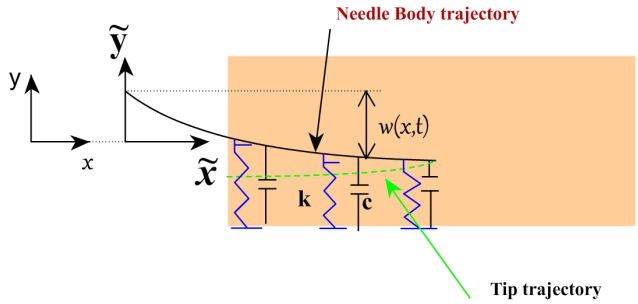

Fig. 8: Mechanism of needle insertion procedures [35]

.

Barb et al. [60] modeled the viscoelastic phase of the insertion forces using KV and HC models. The viscoelastic forces using KV model are expressed as

$$F = \begin{cases} -(Kp + Bv) & if \quad p > 0 \\ 0 & if \quad p \leq 0 \end{cases}$$

where F represents the force exerted on the tissue, v and p are the velocity and position of the needle tip respectively, K and B are stiffness and damping coefficients of the model respectively.

The viscoelastic forces using HC model are expressed as

$$F = \begin{cases} -(\mu p^n + \lambda p^n v) & if \quad p > 0 \\ 0 & if \quad p \leq 0 \end{cases}$$

where n and λ are material parameters.

With comparative tests between the HC and KV models, they concluded that the HC model is more appropriate for computation in visco-elastic cases. The force reconstruction has an error and absolute mean of 0.0194 N and a standard deviation of 0.0125 N.

According to the HC model, the total interaction force on the needle is expressed as

$$F_{tot} = -\mu p_s^n - \lambda p_s^n (v_s - v) + F_f + F_c$$

where F_f is the dry frictional force and F_c is the cutting force applied on the needle. Since the parameters λ and n can't be same, they have identified a simple model and named it as KV generalized model. This model has parameter K, B and they are time varying which are dependent on position and velocity.

Asadian et al. [44] modeled the needle insertion forces in two phases: one, the force during insertion and the other during retraction. They modeled these forces based on the LuGre model wherein they assume insertion velocity to be constant and, that these forces are dependent on the depth of penetration of the needle. They modeled the needle-tissue interaction forces using nonlinear dynamics based on the LuGre model. They implemented an identification procedure which enables the tuning of model parameters according to the tissue properties. Asadian [68] has further studied the effect on tissue behavior and the possible friction models.

This article has been accepted for publication in a future issue of this journal, but has not been fully edited. Content may change prior to final publication. Citation information: DOI 10.1109/RBME.2017.2706966, IEEE Reviews in Biomedical Engineering

Kikuuwe et al. [69] modeled needle insertion and withdrawal using the Coulomb friction model. They initially designed a 1D model and extended it to a 3D model by considering the motion and forces acting in the axial direction. This work is an extension of their previous work where they studied the frictional force corresponding to the change in the direction and depth of the needle [70]. Fukushima et al. [53] studied the frictional force during needle insertion and estimated the needle tip force as the difference between the total insertion force and the frictional force.

A novel shape matching method was used for tissue modeling by Tian et al. [71]. This method has the advantage of numerical stability. The needle is modeled with a flexible virtual needle, and the forces are formulated as the gradient of potential energy. They modeled the forces for both needle insertion and retraction.

VI. Friction Models

The needle-tissue interaction force includes cutting force, stiffness force, and frictional force. The frictional force is the major component of these three forces because the other two forces are acting as point loads whereas the frictional force is a distributed load. It acts along the length of the needle shaft during the entire process of needle insertion and also during withdrawal.

Friction: Friction is the resisting force to the relative motion between two surfaces in contact. One classification of different types of friction is dry friction, fluid friction, internal friction and so on. Dry friction which is a resistive force between two solid surfaces in contact is the combination of static and kinetic friction.

A. Static models

Classical models: Classical friction models consist of different basic models, most of them considering only a single aspect of frictional force [72].

1) Coulomb Friction: The most basic friction model is the Coulomb friction model. The main assumption of this model is that the magnitude of friction is independent of the sliding velocity and contact area. According to this, friction has two regimes: static, and kinetic. Static friction at zero velocity is when the force can take any of a range of values and, it opposes the impending motion. Kinetic friction occurs for nonzero velocities, and it opposes the actual motion as shown in Fig. 9 [73]. It is constant in magnitude and equal to the normal force multiplied by a constant coefficient times the sign of the velocity. It is described as

$$F = F_c sgn(v)$$

where F_c is frictional force which is proportional to normal load (F_N) i.e., $F_c = \mu F_N$ and μ is the proportionality constant.

Coulomb's model accurately portrays the kinetic friction but, the transition from static to kinetic friction is unrealistic as the discontinuity at zero displacement implies an infinite rate of change of force that is not physically possible.

The major drawback of the Coulomb friction model is the uncertainity at zero velocity [74].

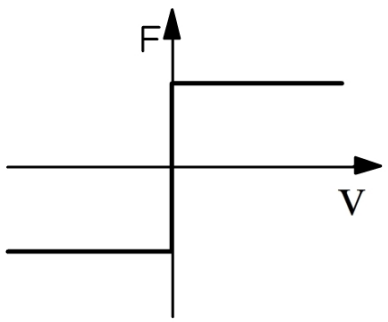

Fig. 9: Coulomb friction [73]

.

2) Viscous Friction: Viscous friction is one of the classical models which has viscous frictional force as proportional to the sliding velocity [75] as shown in Fig. 10:
when

$$v(t) \neq 0 : F_f(t) = -F_v v(t)$$

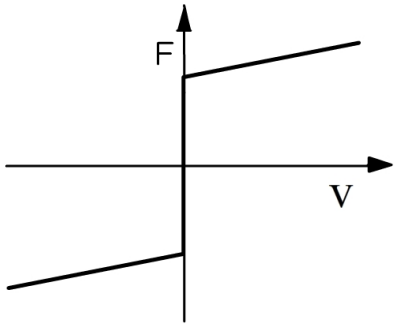

Fig. 10: Viscous friction [73]

.

3) Static Friction: Static friction represents the frictional force at rest or zero sliding velocity. Lee et al. [76] studied the magnitude of frictional force at different velocities and observed that frictional force at rest is higher than coulomb frictional force at nonzero velocity, as shown in Fig. 11. Static friction has a threshold force value above which the object starts moving as shown in Fig. 12. The friction force at rest is a function of external forces but, not the sliding velocity of the object. This can be modeled as

When $v(t) = 0$:

$$F_f(t) = \begin{cases} F_e & |F_e| < F_s \\ F_s sgn(F_e) & |F_e| > F_s \end{cases}$$

where F_s is the static frictional force, F_e is the external force.

4) Stribeck Effect: Stribeck noticed a negatively-sloped and nonlinear friction-velocity characteristic at low velocities for more lubricated and some dry contacts. This negatively-sloped curve gives an important contribution to stick and slip. Because of dynamic friction effects, instantaneous friction is not only a function of instantaneous velocity but also a function of the history of the velocity [77]. The friction at steady state velocity gives the Stribeck curve, as shown in Fig.13.

This article has been accepted for publication in a future issue of this journal, but has not been fully edited. Content may change prior to final publication. Citation information: DOI 10.1109/RBME.2017.2706966, IEEE Reviews in Biomedical Engineering

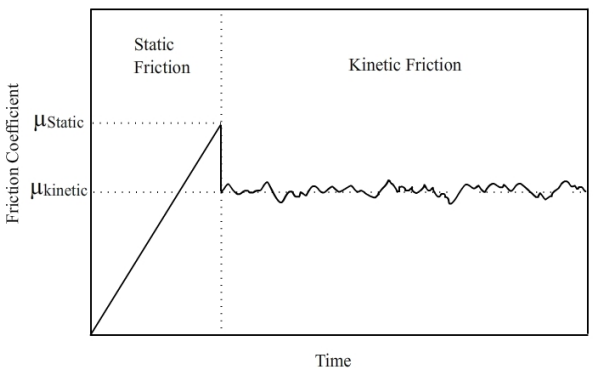

Fig. 11: Static and kinetic friction [76]

.

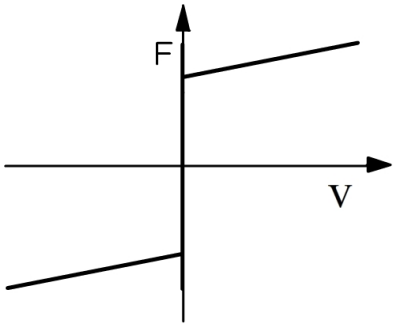

Fig. 12: Static friction with the combination of viscous and coulomb friction [73]

.

$$F_f(t) = \begin{cases} F(v) & if\ v \neq 0 \\ F_e & if\ v = 0\ and\ |F_e| < F_s \\ F_s sgn(F_e) & otherwise \end{cases}$$

A common form of non-linearity is

$$F(v) = F_c + (F_s - F_c)e^{-\left|\frac{v}{V_\sigma}\right|^{\delta\sigma}} + F_v v$$

V_σ is called the Stribeck velocity.

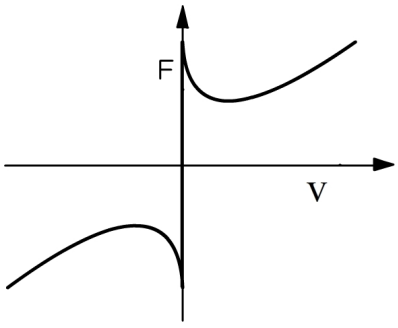

Fig. 13: Stribeck curve characteristics [76]

.

The main drawback of the Coulomb, Viscous, and Stribeck friction models is the uncertainty of the friction force at zero velocity [78].

5) Karnopp model (derived from coulomb's model): In this model, Karnopp [79] has rectified the frictional force uncertainty by considering a pseudo-velocity *p(t)* for an interval of $\pm D_v$ at the neighborhood of zero velocity where the velocity is assumed to be zero. The pseudo-velocity *p(t)* is not explicitly a velocity parameter but, considered as momentum by Karnopp. The rate of change of p(t) is the difference between the modeled frictional force and the force acting on the system.

$$\dot{p}(t) = [F_a(t) - F_m(t)]$$

where F_a is described as the force applied to the system, F_m is described as modeled frictional force.

The velocity parameter of the model is formulated as:

$$v(t) = \begin{cases} 0 & |p(t))| < D_v \\ \frac{1}{M}p(t) & |p(t))| \geq D_v \end{cases}$$

where *M* is described as the mass of the entire system.

The friction law is given as:

$$F_m(v(t), F_a(t)) =$$
$$\begin{cases} -sgn[f_a(t)]max[|F_a(t)|, (F_c + F_s)] & |v(t)| < D_v \\ -sgn[v(t)]F_c + F_v v(t) & |v(t)| \geq D_v \end{cases}$$

where F_c, F_s, and F_v are described as Coulomb, static, and viscous frictional force respectively.

Romano and Garcia [80] applied Karnopp model for the control of the valve. The main drawbacks of Karnopp model are consideration of pseudo velocity which is not applicable for system-level studies and its applications, it is not appropriate for real-time systems and, the external force given to the system is not always definite.

B. Dynamic friction

1) Pre-sliding Displacement (first studied by Dahl): It is the displacement of rolling or sliding contacts prior to true sliding. It arises due to the plastic and/or elastic deformation of the contacting asperities. It is the initial 1–50 μm displacement.

$$F_f(x) = -K_t x$$

where $F_f(x)$ is described as the frictional force in terms of pre-sliding displacement, K_t is a constant, the stiffness coefficient of the material and *x* is displacement.

2) Rising Static Friction and dwell time: At breakaway, the magnitude of static friction, λ_b, is not constant. When there is no motion, the static friction builds with time from a reduced value to its ultimate steady state value which is also known as stiction force, as shown in Fig. 11 (It depends on the time spent at zero velocity).

The Armstrong model which follows the above phenomenon is:

$$F_{s,p_n}(\gamma, t_d) = F_{S,p_{n-1}} + (F_{s,\infty} - F_{S,p_{n-1}} \frac{t_d}{(t_d + \gamma))}$$

where F_{s,p_n} is the magnitude of static friction at the breakaway i.e., the start of n^{th} interval of slip, $F_{S,p(n-1)}$ is the magnitude of static friction at the start of $(n-1)^{th}$ interval of slip, $F_{s,\infty}$ is the maximum static friction possible, γ is an empirical parameter, static friction rise time.

This article has been accepted for publication in a future issue of this journal, but has not been fully edited. Content may change prior to final publication. Citation information: DOI 10.1109/RBME.2017.2706966, IEEE Reviews in Biomedical Engineering

3) Frictional Memory: It is the time delay observed between changes in frictional force to that of changes in the velocity or the normal load [81], [82]. Rabinowicz [83] proposed the time delay of frictional response as memory dependent with the consideration of the hysteresis loop generated during the increasing and decreasing velocities, as shown in Fig. 14.

Instantaneous friction is a function of sliding velocity and load. It is modeled as a time lag:

$$F_f(t) = F_{vel}(v(t - \delta t))$$

where $F_f(t)$ is the frictional force at an instant, $F_{vel}(\cdot)$ is friction in terms of steady state velocity and δt is the delay term.

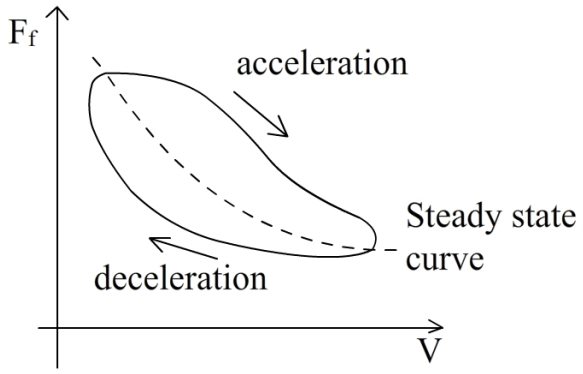

Fig. 14: Hysteresis in the frictional force for relative velocity [84]

.

4) Seven parameter model: This is the first model which includes the seven different basic friction elements, viz. coulomb, viscous, static, stribeck, dwell time, pre-sliding displacement, and frictional memory [66]. The pre-sliding displacement element is modeled using a separate equation, thereby having two equations, one for the stiction phenomenon where velocity is zero and, the other for the sliding phenomenon where velocity is nonzero. The transition between these two phenomena is governed by a certain mechanism. The frictional phenomenon is modeled as:

when sticking,

$$F(x) = \sigma_0 x$$

when sliding,

$$F(v,t) = (F_c + F_s(\gamma, t_d)\frac{1}{(\frac{1+(v(t-\tau_e)}{v_s})^2})sgn(v) + F_v v$$

where

$$F_s(\gamma, t_d) = F_{S,a} + (F_{s,\infty} - F_{S,a}\frac{t_d}{(t_d + \gamma)})$$

$F_{S,a}$ is the Stribeck friction at an instant 'a'.

t_d is dwell time, which is the time spent at a certain stage of the process.

The main drawback of this model is that the switching mechanism between the stiction phase to the sliding phase is not specified. In this model, the Stribeck friction parameter is considered with a velocity after a certain time, γ.

5) Dahl Model: The main advantage of this model over other dynamic models is the ability to perform control system simulations. Dahl proposed an analogy between frictional behavior and the stress-strain property.

According to Dahl [85], objects subjected to small and large displacements are compared to the elastic and plastic deformation respectively; maximum stress in a stress-strain curve is compared to stiction force. The stress-strain curve for the ductile material is compared to coulomb friction.

With his analogy, the stress-strain curve is modeled using a differential equation as

$$\frac{dF}{dx} = \sigma(1 - \frac{F}{F_c sgn(v)})^\alpha$$

where *F* is the frictional force, F_c is the coulomb force, *x* is the displacement, σ is the stiffness constant and α determines the slope of the stress-strain curve.

This model is an extension of the Coulomb friction model, where the frictional force is not only a function of displacement but also a function of velocity [86]. The above Dahl model is modified as

$$\frac{dF}{dt} = \frac{dF}{dx}\frac{dx}{dt} = \frac{dF}{dx}v = \sigma(1 - \frac{F}{F_c sgn(v)})^\alpha v$$

Bliman [87] studied the model of Dahl mathematically and proved the link between the Dahl model and Coulomb's model. He also coupled the equation of motion with Dahl's model.

Dahl's model captures the pre-displacement and hysteresis phenomena in a dynamic model but, fails to simulate the Stribeck effect, stiction, and the stick-slip phenomenon.

6) LuGre Model: The LuGre model is a collaborative work of Lund and Grenoble which is an extension of the Dahl model [88]. It overcomes one of the disadvantages of the Dahl model by simulating the Stribeck effect. This model is an integrated dynamic friction model which is not possible in the seven-parameter model. It is a six-parameter model which includes the static model elements like coulomb, static, viscous, stribeck friction, frictional memory, and pre-sliding displacement [89]. In the LuGre model friction induces hysteresis in the spring damper system. The instantaneous friction F_f is modeled as:

$$F_f(t) = \sigma_0(t) + \sigma_1(dz(t)/dt) + F_v v(t)$$

where σ_0 is a characteristic stiffness for spring like behavior for small displacements, and σ_1 is a damping parameter. The variable *z(t)* represents the average deflection between two surfaces at an instant *t* which is the friction state. The formulation parameters gets updated according to:

$$dz(t))/dt = v(t) - \sigma_0/g(v(t))z(t)\,|v(t)|$$

where

$$g(v(t)) = F_c + F_s e^{(-(\frac{v}{v_s})^2}$$

F_v, F_s and F_c are static, Stribeck and Coulomb friction respectively. The steady state friction is as follows:

$$F_{ss}(t) = g(v(t)) + F_v v(t)$$

The main advantage of this model is that its formulation can be valid for both rotational and linear coordinates.

This article has been accepted for publication in a future issue of this journal, but has not been fully edited. Content may change prior to final publication. Citation information: DOI 10.1109/RBME.2017.2706966, IEEE Reviews in Biomedical Engineering

Piatkowski [90] studied the effect of the Dahl and LuGre models on pre-sliding displacement. He also studied the effect of velocity on the frictional hysteresis loop. Ashwini [38] studied the impact of the LuGre model on friction-induced hysteresis in the system. Her experimental set-up is modeled based on the Dahl, LuGre, and Maxwell slip models.

Fukushima et al. [53] studied the characteristics of needle tip forces during the needle insertion and designed frictional force estimation method. They estimated the needle tip force by measuring the frictional force during needle insertion. They evaluated the needle tip force as the difference between total insertion force and the frictional force. They modeled the total insertion force and also the frictional force for a single layer and validated with the experimental results.

VII. Experimentation of needle simulators

Hing and Brooks [17] conducted an experiment to get a quantitative measure of the needle forces in 6 DOF. The parameters such as duration of needle insertion, various internal events, and the start of kinetic friction during the withdrawal of the needle were extracted from the two c-arm fluoroscopy set-up. They followed a novel approach for measuring the 3D movement of the beads being placed in brachytherapy in real time. They placed forty 1-mm diameter stainless steel beads which easily show up in X-ray imaging. The fluoroscope set-up would help to track the fiducial markers and the needle during insertion.

Barb et al. [60] designed an instrumented needle as shown in Fig. 15 with a force sensor of 1 DOF along with the sensible phantom. They used these quantitative measures to validate their models described in the earlier sections.

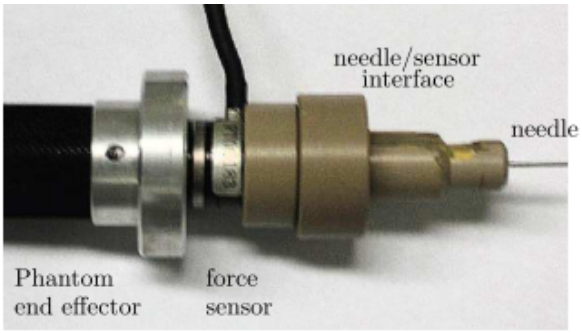

Fig. 15: Instrumented Needle along with with a 1-DOF force sensor [60]

.

Vidal et al. [91] developed a real-time and robust needle simulator with two Phantom Omni. A hybrid volume haptic rendered ultrasound transducer and a volume haptic model were developed for needle puncture. Force measurements were made on real tissues, and these forces are used for modeling. Along with the force data, they used data from CT scan of a particular patient for a patient specific model.

Lehmann et al. [37] conducted an experiment of a needle insertion procedures using a robotic system developed by them as shown in Fig. 16. It is designed with 2 DOF, the translational motion is along the needle axis and, rotational motion is about the needle axis. This system also helps in conducting a manual insertion procedure. The main advantage of their system is its high precision and low friction. Force sensors in 6 DOF (3 DOF forces and 3 DOF torques) are used to measure the insertion forces during needle insertion in the tissue samples. They performed various experiments for manual and automated needle insertion at different velocities for two homogeneous tissue samples. They studied the effect of the rotation of a needle by 180^0 by performing an experiment with the help of a virtual sensor.

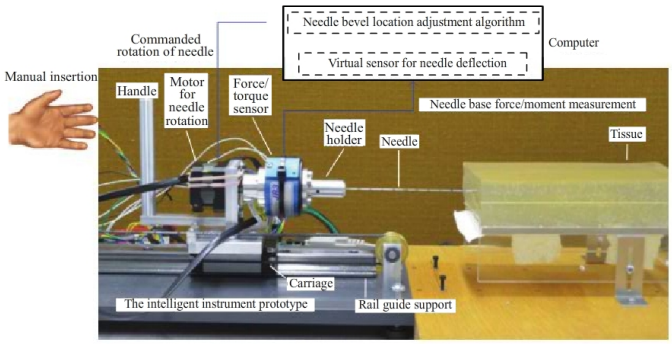

Fig. 16: Instrumental needle setup for both automated and manual insertion [37]

.

Wei et al. [92] experimented on the needle insertion forces for different depths as shown in Fig. 17a and, they also studied the effect of insertion depth on needle deflection as shown in Fig. 17b. Their experimental set-up includes a needle which is mounted on a digital force–measuring gauge that measures force and torques in 1 DOF. They also used an X-ray fluoroscopic system for observing the mounting conditions in the system. Their study concluded that the difference in the insertion force in two samples is due to internal structures such as blood vessels. Their study also concluded that the needle gets deflected to less than 1^0 after a certain depth is attained.

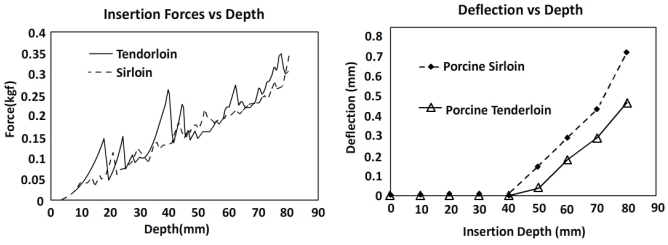

(a) Insertion force (b) Needle deflection

Fig. 17: Experimental results for porcine samples [92]

Daykin and Bacon [93] designed and constructed an epidural simulator for teaching the skills to trainees. They also incorporated the loss of resistance to injection in the simulator which is a major challenge for the novice. Resistance to needle movement is simulated with two spring loaded friction plates. The major disadvantage of this simulator is that it can operate in only 1 DOF. Tran et al. [94] studied the injection

This article has been accepted for publication in a future issue of this journal, but has not been fully edited. Content may change prior to final publication. Citation information: DOI 10.1109/RBME.2017.2706966, IEEE Reviews in Biomedical Engineering

flow rate for different layers during needle insertion, such as muscle, interspinous ligament, and ligamentum flavum. Shin et al. [95] developed a 2 DOF needle simulator with high-quality haptic feedback with no power loss. Dang et al. [96] used a 3 DOF force feedback device, Phantom, to develop an epidural simulator. They incorporated an additional DOF by simulating the loss of resistance in the simulator. Bibin et al. [97] developed a regional anesthesia simulator in a virtual environment with realistic 3D anatomical models. Grottke et al. [98] developed a virtual reality–based regional anesthesia training simulator with the consideration of advantages such as improper feedback from the tissue layers, inter-patient variability, and repeated use over manikin-based simulators.

Vaughan et al. [99] have reviewed the available epidural and lumbar simulators and also discussed the strengths and weaknesses of these simulators. Many other researchers have performed various experiments on needle insertion procedures such as the study of needle diameter [49], [100]; insertion depth; insertion velocity [50]; insertion forces; and needle deflection [35]. Some of the experiments were performed to validate the models and to measure the tissue stiffness [101].

VIII. Psychophysics

As a human is involved in the process of manual needle insertion, the forces she encounters during the insertion are the physical stimulus and the sensation of these forces which she is experiencing need to be measured because she is controlling the forces. As there is no literature on needle insertion including on humans as a part of the system, in this section we briefly introduce psychophysics and explain how psychophysics is useful in needle insertion, experiments, modeling, and simulation for training.

The study of the relationship between the stimulus (a physical phenomenon) and sensation (an attribute of the sensory system) is psychophysics. Therefore, the problems of psychophysics represent the basic problems of modern psychology [102]. All the human senses (sight [103], [104]; hearing [105], [106]; taste [107], [108]; smell [109], [110]; touch [111]–[115]; and also sense of time) have been studied in the correspondence of psychophysical parameters. The experiments that are implemented using psychophysics relate to the two parameters, the sensation, and physical stimulus, wherein the subject would experience the sensation based on the stimulus specifications provided for that experiment. Lawrence et al. [116] studied the effect of friction that is inherent in haptic interfaces on human perception. Despite the study of the sensory system, there are three other main areas of study: absolute threshold, discrimination thresholds, and scaling, which result in the detection, discrimination, and scaling of the stimuli respectively [117].

One of the applications of this psychophysical study is to quantify the clinical skills. The clinical skills invariably require hand-eye coordination, which involves the human haptic system (both human sensory system and motor system). The psychophysical study of both the sensory and motor systems can provide us with the limitations on sensing and controlling the forces during needle insertion and thereby designing a better training system. In this section, we cite some of the related psychophysical experiments in medical simulators that may be indirectly used to quantify needle insertion skills.

Neil and Sarah [113] did a comparative study on identification of stiffness by veterinarians and novices. They considered a virtually rendered stiffness of five levels in the range of 0.2–0.5 N/mm. Their results prove that veterinarians performed appreciably (100%) better than novices. They also suggest that quantifying the skills of clinicians would help in improving the training methods for the novices. Therefore, similar psychophysical experiments can be performed to examine the performance level of novices after the training. Nisky and Pressman [118] studied the effect of delay in telesurgery where stiffness needs to be controlled. They explored the interaction between the device (Phantom Premium 1.5) and generated a force field that approaches the properties of real tissues. They performed the experiment in four phases: null training, base training, task training, and a test phase where the task of the experiment is to differentiate the stiffness of the force field. Nisky et al. have also explored similar experiments and studied the perception and action on teleoperated needle insertion procedures [119]. Brelstaff et al. [120] have demonstrated psychophysical experiments for both visual and haptic effects. Their experiment performed on the virtual bone with the incorporation of the elastic and erosion properties of real bone addressed both surface probing and interior drilling tasks. Their study was to explore the skills which were trained using their bone burring simulator. Gerovich et al. [121] studied the effect of visual and haptic feedback on human performance by conducting an experiment using a 1 DOF needle simulator and concluded that force feedback might not be necessary until the visual feedback is limited. Klymenko and Pizer [103] explored psychophysical experiments on the subjects' performance evaluation, particularly to the observers' sensitivity to visual parameters. The experiment was to detect the sensitivity to medical imaging parameters (visual threshold).

Since it is uncommon in medical simulators to have sensors connected to the subject to quantitatively measure all the required thresholds and differential thresholds for each parameter, it is a good practice to perform psychophysical experiments that improve the level of training.

In the case of the needle simulators, the psychophysical experiments help to study various parameters, and some of the psychophysical parameters in literature relevant to the needle insertion procedures are:

1) The threshold forces applied by the doctors at different layers of the insertion procedure,

- Typical range of force for single finger is 1 N to 10 N, maximum controllable range is up to 100 N, Control resolution 0.05 to 0.5 N, range of force during grasping is 50 N to 100 N [122].
- Contact force resolution is 5-15 % of the reference value [123].
- Force detection threshold between index, middle, pinkie and multi-finger interaction are 33.5, 32.1, 33.5, 28.9 mN respectively but less sensitivity with the ring finger (mean threshold of 43.6 mN) [124]

- JND for pinching motions between finger and thumb is 5-10 % with a constant resisting force of 2.5 N to 10 N [125].
- Force JND for left and right index finger is approximately 10 % of the reference value [126].
- Bandwidth for sensory system is 20 to 30 Hz [127].
- Bandwidth for limb motions depends on the mode of operation [127]:
  - Bandwidth for periodic signals 2-5 Hz.
  - Bandwidth for internally generated or known trajectories is up to 5 Hz.
  - Bandwidth for unexpected signals is 1-2 Hz. and
  - Bandwidth for reflex actions is about 10 Hz.

2) Tissue stiffness at each layer,

3) Just noticeable difference (JND) in terms of the orientation of the needle during insertion, and

- The JND of human sensitivity to rotation or in orientation sensing is [122]
  1) Resolution for finger joints is 2.5^0
  2) Resolution for the wrist and elbow joints is 2^0, and
  3) Resolution for the shoulder joint is about 0.8^0.

4) Threshold velocity with which the needle is being inserted into the tissues.

- Velocity JND or resolution at fingertip and wrist are 0.1 m/s and 1 m/s respectively [122].

This psychophysical parameter analysis would help in improving the design of simulators and simplify the models [128]. The parameters mentioned above such as human force resolutions, force thresholds, bandwidth, and velocity can be used to design a model whereas the Just Noticeable Difference (JND) of joint rotations and range of motion can be used to develop the simulator. Thus, to improve human performance, haptic devices have to be designed by considering quantitative human studies [129] and training methods and help the trainees with a better experience. Jones and Tan [130] reviewed the applications of psychophysical parameters on haptics.

IX. Summary

In this paper, we have described state-of-the-art needle insertion modeling in soft tissues. Modeling of needle insertion is classified into needle insertion forces, tissue deformation, and needle-tissue interaction and each of the models was discussed in great detail. In particular, the classical friction models which are neglected in the literature were also emphasized. Several experimental techniques or simulators for needle insertion procedures were described, psychophysical analysis of the human sensations during the operation of a needle insertion simulator which is the future of research in needle insertion procedures were also discussed in detail.

The study of different models found that the total interaction forces were the combination of cutting force, friction force, and sliding force. The consideration of forward and backward kinematics made them enable both needle path planning and path correction. It is also found that most of the models assumed constant velocity during the needle insertion procedures. Frictional models (both classical or static models and dynamic frictional models) which were neglected in the literature were also discussed. It is well known that human tissues have nonlinear and viscoelastic properties. Therefore, classical or static models are not accurate in incorporating all the mechanical properties of biological tissues. In the literature, only a few dynamic models are used for modeling needle procedures in human tissues, like the LuGre model. A few experiments in the literature to study the effect of delay in perception and action in teleoperated needle procedures and teleoperated surgeries have found that delay causes inaccurate estimation of tissue stiffness. It is shown that these psychophysical experiments are necessary to enhance the training methods by improving the accuracy of the models and thereby the skills of the trainee.

References

[1] R. Alterovitz, A. Lim, K. Goldberg, G. S. Chirikjian, and A. M. Okamura, "Steering flexible needles under Markov motion uncertainty," 2005 IEEE/RSJ International Conference on Intelligent Robots and Systems, IROS, pp. 120–125, 2005.

[2] J. B. Ra, S. M. Kwon, J. K. Kim, J. Yi, K. H. Kim, H. W. Park, K. U. Kyung, D. S. Kwon, H. S. Kang, S. T. Kwon, L. Jiang, J. Zeng, K. Cleary, and S. K. Mun, "Spine needle biopsy simulator using visual and force feedback," Computer Aided Surgery, vol. 7, no. 6, pp. 353–363, 2002.

[3] E. H. Smith, "Complications of percutaneous abdominal fine-needle biopsy. review.," Radiology, vol. 178, no. 1, pp. 253–258, 1991.

[4] S. Ullrich, O. Grottke, R. Rossaint, M. Staat, T. M. Deserno, and T. Kuhlen, "Virtual needle simulation with haptics for regional anaesthesia," Proc. of the IEEE Virtual Reality 2010, Workshop on Medical Virtual Environments, Waltham, MA, USA, March 21, 2010, pp. 1–3, 2010.

[5] Y. Auroy, D. Benhamou, L. Bargues, C. Ecoffey, B. Falissard, F. Mercier, H. Bouaziz, and K. Samii, "Major Complications of Regional Anesthesia in France The SOS Regional Anesthesia Hotline Service," Anesthesiology, vol. 97, no. 5, pp. 1274–80, 2002.

[6] C. Konrad, G. Schüpfer, M. Wietlisbach, and H. Gerber, "Learning manual skills in anesthesiology: Is there a recommended number of cases for anesthetic procedures?," Anesthesia and analgesia, vol. 86, no. 3, pp. 635–639, 1998.

[7] C. Hellekant, "Vascular complications following needle puncture of the liver. Clinical angiography.," Acta radiologica: diagnosis, vol. 17, pp. 209–22, mar 1976.

[8] C. Basdogan, S. De, J. Kim, M. Manivannan, H. Kim, and M. A. Srinivasan, "Haptics in minimally invasive surgical simulation and training," IEEE computer graphics and applications, vol. 24, no. 2, pp. 56–64, 2004.

[9] M. S. Raghu Prasad, M. Manivannan, and S. M. Chandramohan, "Effects of laparoscopic instrument and finger on force perception: a first step towards laparoscopic force-skills training," Surgical Endoscopy and Other Interventional Techniques, pp. 1927–1943, 2014.

[10] C. Cope, "Needle endoscopy in special procedures.," Radiology, vol. 168, pp. 353–8, aug 1988.

[11] M. Marchal, E. Promayon, and J. Troccaz, "Comparisons of needle insertion in brachytherapy protocols using a soft tissue discrete model," in Surgetica 2007, pp. pp–153, Sauramps Medical, 2007.

[12] S. J. Damore, A. N. Syed, A. A. Puthawala, and A. Sharma, "Needle displacement during hdr brachytherapy in the treatment of prostate cancer," International Journal of Radiation Oncology* Biology* Physics, vol. 46, no. 5, pp. 1205–1211, 2000.

[13] P. D. Grimm, "Precision implant needle and method of using same in seed implant treatment of prostate cancer," Aug. 17 1999. US Patent 5,938,583.

[14] R. D. Miller, L. I. Eriksson, L. A. Fleisher, J. P. Wiener-Kronish, N. H. Cohen, and W. L. Young, Miller's anesthesia. Elsevier Health Sciences, 2014.

[15] C. W. Kim, K. Siemionow, D. G. Anderson, and F. M. Phillips, "The current state of minimally invasive spine surgery," J Bone Joint Surg Am, vol. 93, no. 6, pp. 582–596, 2011.

[16] W. J. Dyche, J. H. Walsh, and J. A. Nelson, "An acls laboratory rotation for undergraduate medical students," Annals of emergency medicine, vol. 12, no. 4, pp. 208–211, 1983.

[17] J. T. Hing, a. D. Brooks, and J. P. Desai, "Reality-based needle insertion simulation for haptic feedback in prostate brachytherapy," Proceedings 2006 IEEE International Conference on Robotics and Automation 2006 ICRA 2006, no. May, pp. 619–624, 2006.

[18] M. Torabi, K. Hauser, R. Alterovitz, V. Duindam, and K. Goldberg, "Guiding medical needles using single-point tissue manipulation," Proceedings - IEEE International Conference on Robotics and Automation, pp. 2705–2710, 2009.

[19] N. Chentanez, R. Alterovitz, D. Ritchie, L. Cho, K. K. Hauser, K. Goldberg, J. R. Shewchuk, and J. F. O'Brien, "Interactive simulation of surgical needle insertion and steering," ACM Transactions on Graphics, vol. 28, no. 3, p. 1, 2009.

[20] N. Abolhassani, R. Patel, and M. Moallem, "Needle insertion into soft tissue: A survey," Medical Engineering and Physics, vol. 29, no. 4, pp. 413–431, 2007.

[21] R. S. Haluck, W. Murraya, R. Webster, N. Mohler, and M. Melkonian, "A haptic lumbar puncture simulator," Proceedings of Medicine Meets Virtual Reality (MMVR'2000), 2000.

[22] L. B. Ready, "Acute pain: Lessons learned from 25,000 patients," Regional Anesthesia and Pain Medicine, vol. 24, no. 6, pp. 499–505, 1999.

[23] R. Taschereau, J. Pouliot, J. Roy, and D. Tremblay, "Seed misplacement and stabilizing needles in transperineal permanent prostate implants," Radiotherapy and Oncology, vol. 55, no. 1, pp. 59–63, 2000.

[24] C. Sutherland, K. Hashtrudi-Zaad, R. Sellens, P. Abolmaesumi, and P. Mousavi, "An augmented reality haptic training simulator for spinal needle procedures," IEEE Transactions on Biomedical Engineering, vol. 60, no. 11, pp. 3009–3018, 2013.

[25] M. M. Hammoud, F. S. Nuthalapaty, A. R. Goepfert, P. M. Casey, S. Emmons, E. L. Espey, J. M. Kaczmarczyk, N. T. Katz, J. J. Neutens, E. G. Peskin, et al., "To the point: medical education review of the role of simulators in surgical training," American journal of obstetrics and gynecology, vol. 199, no. 4, pp. 338–343, 2008.

[26] D. Escobar-Castillejos, J. Noguez, L. Neri, A. Magana, and B. Benes, "A review of simulators with haptic devices for medical training," Journal of medical systems, vol. 40, no. 4, pp. 1–22, 2016.

[27] P.-J. Fager, "The use of haptics in medical applications," The International Journal of Medical Robotics and Computer Assisted Surgery, vol. 1, no. 1, pp. 36–42, 2004.

[28] C. Basdogan, S. De, J. Kim, M. Muniyandi, H. Kim, and M. A. Srinivasan, "Haptics in minimally invasive surgical simulation and training," IEEE computer graphics and applications, vol. 24, no. 2, pp. 56–64, 2004.

[29] T. R. Coles, D. Meglan, and N. W. John, "The role of haptics in medical training simulators: A survey of the state of the art," IEEE Transactions on haptics, vol. 4, no. 1, pp. 51–66, 2011.

[30] S. Ullrich and T. Kuhlen, "Haptic palpation for medical simulation in virtual environments," IEEE Transactions on Visualization and Computer Graphics, vol. 18, no. 4, pp. 617–625, 2012.

[31] S. DiMaio and S. Salcudean, "Needle insertion modeling and simulation," IEEE Transactions on Robotics and Automation, vol. 19, pp. 864–875, oct 2003.

[32] D. De Lorenzo, Y. Koseki, E. De Momi, K. Chinzei, and A. M. Okamura, "Coaxial needle insertion assistant with enhanced force feedback," IEEE Transactions on Biomedical Engineering, vol. 60, no. 2, pp. 379–389, 2013.

[33] O. Goksel, K. Sapchuk, and S. E. Salcudean, "Haptic simulator for prostate brachytherapy with simulated needle and probe interaction," IEEE Transactions on Haptics, vol. 4, pp. 188–198, May 2011.

[34] S. P. DiMaio and S. E. Salcudean, "Interactive simulation of needle insertion models," IEEE Transactions on Biomedical Engineering, vol. 52, no. 7, pp. 1167–1179, 2005.

[35] K. Yan, W. S. Ng, K. V. Ling, Y. Yu, T. Podder, T. I. Liu, and C. Cheng, "Needle steering modeling and analysis using unconstrained modal analysis," Proceedings of the First IEEE/RAS-EMBS International Conference on Biomedical Robotics and Biomechatronics, 2006, BioRob 2006, vol. 2006, pp. 87–92, 2006.

[36] D. Glozman and M. Shoham, "Flexible needle steering for percutaneous therapies.," Computer aided surgery : official journal of the International Society for Computer Aided Surgery, vol. 11, no. 4, pp. 194–201, 2006.

[37] T. Lehmann, M. Tavakoli, N. Usmani, and R. Sloboda, "Force-sensor-based estimation of needle tip deflection in brachytherapy," Journal of Sensors, vol. 2013, no. Figure 2, 2013.

[38] A. K. Padthe, J. Oh, and D. S. Bernstein, "On the lugre model and friction-induced hysteresis," in Proceedings of the 2006 American Control Conference, Minneapolis, Minnesota, USA, vol. 3247, p. 3252, 2006.

[39] C. Simone and A. Okamura, "Modeling of needle insertion forces for robot-assisted percutaneous therapy," Proceedings 2002 IEEE International Conference on Robotics and Automation, vol. 2, no. May, pp. 2085–2091, 2002.

[40] P. N. Brett, T. J. Parker, A. J. Harrison, T. A. Thomas, and A. Carr, "Simulation of resistance forces acting on surgical needles.," Proceedings of the Institution of Mechanical Engineers. Part H, Journal of engineering in medicine, vol. 211, no. 4, pp. 335–47, 1997.

[41] K. Naemura, A. Sakai, T. Hayashi, and H. Saito, "Epidural insertion simulator of higher insertion resistance & drop rate after puncture.," Conference proceedings : Annual International Conference of the IEEE Engineering in Medicine and Biology Society. IEEE Engineering in Medicine and Biology Society. Conference, vol. 2008, pp. 3249–52, 2008.

[42] D. J. van Gerwen, J. Dankelman, and J. J. van den Dobbelsteen, "Needle-tissue interaction forces - A survey of experimental data," Medical Engineering and Physics, vol. 34, no. 6, pp. 665–680, 2012.

[43] V. N. Dubey, M. Y. Wee, N. Vaughan, and R. Isaacs, Biomedical Engineering in Epidural Anaesthesia Research. INTECH Open Access Publisher, 2013.

[44] A. Asadian, M. R. Kermani, and R. V. Patel, "A compact dynamic force model for needle-tissue interaction.," Conference proceedings : ... Annual International Conference of the IEEE Engineering in Medicine and Biology Society. IEEE Engineering in Medicine and Biology Society. Annual Conference, vol. 2010, pp. 2292–5, 2010.

[45] O. Goksel, E. Dehghan, and S. E. Salcudean, "Modeling and simulation of flexible needles," Medical Engineering and Physics, vol. 31, no. 9, pp. 1069–1078, 2009.

[46] H. Kataoka, T. Washio, M. Audette, and K. Mizuhara, "A model for relations between needle deflection, force, and thickness on needle penetration," Lecture Notes in Computer Science (including subseries Lecture Notes in Artificial Intelligence and Lecture Notes in Bioinformatics), vol. 2208, pp. 966–974, 2001.

[47] M. Khadem, B. Fallahi, C. Rossa, R. S. Sloboda, N. Usmani, and M. Tavakoli, "A Mechanics-based Model for Simulation and Control of Flexible Needle Insertion in Soft Tissue," pp. 2264–2269, 2015.

[48] A. M. Okamura, C. Simone, and M. D. O'Leary, "Force modeling for needle insertion into soft tissue.," IEEE transactions on bio-medical engineering, vol. 51, no. 10, pp. 1707–16, 2004.

[49] S. Misra, K. B. Reed, B. W. Schafer, K. Ramesh, and A. M. Okamura, "Mechanics of flexible needles robotically steered through soft tissue," The International journal of robotics research, 2010.

[50] M. Mahvash and P. E. Dupont, "Mechanics of dynamic needle insertion into a biological material," IEEE Transactions on Biomedical Engineering, vol. 57, no. 4, pp. 934–943, 2010.

[51] M. Farber, F. Hummel, C. Gerloff, and H. Handels, "Virtual Reality Simulator for the Training of Lumbar Punctures," Methods of Information in Medicine, vol. 48, pp. 493–501, may 2009.

[52] Y.-c. Fung, Biomechanics: mechanical properties of living tissues. Springer Science & Business Media, 2013.

[53] Y. Fukushima and K. Naemura, "Estimation of the friction force during the needle insertion using the disturbance observer and the recursive least square," ROBOMECH Journal, vol. 1, p. 14, dec 2014.

[54] J. C. Teoh and T. Lee, "The effect of gender, age, bodyweight, height and body mass index on plantar soft tissue stiffness," Journal of Foot and Ankle Research, vol. 7, no. 1, pp. 1–2, 2014.

[55] H. Delingette, "Toward realistic soft-tissue modeling in medical simulation," Proceedings of the IEEE, vol. 86, pp. 512–523, mar 1998.

[56] B. Querleux, Computational Biophysics of the Skin. CRC Press, 2016.

[57] O. Goksel, S. E. Salcudean, and S. P. Dimaio, "3D simulation of needle-tissue interaction with application to prostate brachytherapy.," Computer aided surgery : official journal of the International Society for Computer Aided Surgery, vol. 11, no. 6, pp. 279–88, 2006.

[58] D. Lepiller, M. Sermesant, M. Pop, H. Delingette, G. A. Wright, and N. Ayache, "Medical Image Computing and Computer-Assisted Intervention – MICCAI 2008," Lecture Notes in Computer Science (including subseries Lecture Notes in Artificial Intelligence and Lecture Notes in Bioinformatics), vol. 5241, no. PART 1, pp. 678–685, 2008.

[59] J. Xu, L. Wang, K. C. L. Wong, and P. Shi, "A Meshless Framework For Bevel-tip Flexible Needle Insertion Through Soft Tissue," pp. 753–758, 2010.

[60] L. Barbé, B. Bayle, M. de Mathelin, and A. Gangi, "Needle insertions modeling: Identifiability and limitations," Biomedical Signal Processing and Control, vol. 2, pp. 191–198, jul 2007.

[61] N. Diolaiti, C. Melchiorri, and S. Stramigioli, "Contact impedance estimation for robotic systems," IEEE Transactions on Robotics, vol. 21, no. 5, pp. 925–935, 2005.

[62] L. Wang, Z. Wang, and S. Hirai, "Modeling and simulation of friction forces during needle insertion using Local Constraint Method," IEEE International Conference on Intelligent Robots and Systems, pp. 4926–4932, 2012.

[63] T. C. Gasser, R. W. Ogden, and G. A. Holzapfel, "Hyperelastic modelling of arterial layers with distributed collagen fibre orientations," Journal of The Royal Society Interface, vol. 3, no. 6, pp. 15–35, 2006.

[64] J. A. Weiss, B. N. Maker, and S. Govindjee, "Finite element implementation of incompressible, transversely isotropic hyperelasticity," Computer Methods in Applied Mechanics and Engineering, vol. 135, no. 1, pp. 107 – 128, 1996.

[65] G. Limbert and J. Middleton, "A polyconvex anisotropic strain energy function. application to soft tissue mechanics," ASME Summer Bioengineering Conference, Vali, 2005.

[66] G. Limbert, "A mesostructurally-based anisotropic continuum model for biological soft tissues–decoupled invariant formulation.," Journal of the mechanical behavior of biomedical materials, vol. 4, pp. 1637–57, nov 2011.

[67] E. Dehghan, O. Goksel, and S. E. Salcudean, Medical Image Computing and Computer-Assisted Intervention – MICCAI 2006: 9th International Conference, Copenhagen, Denmark, October 1-6, 2006. Proceedings, Part I, ch. A Comparison of Needle Bending Models, pp. 305–312. Berlin, Heidelberg: Springer Berlin Heidelberg, 2006.

[68] A. Asadian, R. V. Patel, and M. R. Kermani, "Dynamics of translational friction in needle-tissue interaction during needle insertion," Annals of Biomedical Engineering, vol. 42, no. 1, pp. 73–85, 2014.

[69] R. Kikuuwe, Y. Kobayashi, and H. Fujimoto, "Coulomb-friction-based needle insertion/withdrawal model and its discrete-time implementation," in Proceedings of EuroHaptics, pp. 207–212, 2006.

[70] R. Kikuuwe, N. Takesue, A. Sano, H. Mochiyama, and H. Fujimoto, "Fixed-step friction simulation: from classical coulomb model to modern continuous models," in 2005 IEEE/RSJ International Conference on Intelligent Robots and Systems, pp. 1009–1016, IEEE, 2005.

[71] Y. Tian, "Haptic Simulation of Needle-tissue Interaction Based on Shape Matching," 2014.

[72] P. Korondi, J. Halas, K. Samu, A. Bojtos, and P. Tamas, Robot Applications. BME MOGI, 2014.

[73] K. Seeler, System Dynamics, ch. An Introduction for Mechanical Engineers, pp. 0–667. Berlin, Heidelberg: Springer-Verlag New York, 2014.

[74] M. Linderoth, A. Stolt, A. Robertsson, and R. Johansson, "Robotic force estimation using motor torques and modeling of low velocity friction disturbances," in 2013 IEEE/RSJ International Conference on Intelligent Robots and Systems, pp. 3550–3556, Nov 2013.

[75] V. van Geffen, "A study of friction models and friction compensation," DCT, vol. 118, p. 24, 2009.

[76] C.-H. Lee and A. a. Polycarpou, "Static Friction Experiments and Verification of an Improved Elastic-Plastic Model Including Roughness Effects," Journal of Tribology, vol. 129, no. 4, p. 754, 2007.

[77] D. K. Peter, H. Janos, D. S. Krisztian, B. Attila, and D. T. Peter, Robot Applications. BME MOGI, 2014.

[78] S. Andersson, A. Söderberg, and S. Björklund, "Friction models for sliding dry, boundary and mixed lubricated contacts," Tribology International, vol. 40, pp. 580–587, apr 2007.

[79] D. Karnopp, "Computer Simulation of Stick-Slip Friction in Mechanical Dynamic Systems," Journal of Dynamic Systems, Measurement, and Control, vol. 107, no. 1, p. 100, 1985.

[80] R. A. Romano and C. Garcia, "Karnopp Friction Model Identification for a Real Control Valve," in IFAC Proceedings Volumes, vol. 41, pp. 14906–14911, 2008.

[81] B. Armstrong-Helouvry, "Frictional memory in servo control," in Proceedings of 1994 American Control Conference - ACC '94, vol. 2, pp. 1786–1790, IEEE, 1994.

[82] H. Olsson, K. J. Astrom, C. C. De Wit, M. Gafvert, and P. Lischinsky, "Friction models and friction compensation," European journal of control, vol. 4, no. 3, pp. 176—-195, 1998.

[83] E. Rabinowicz, "The Intrinsic Variables affecting the Stick-Slip Process," Proceedings of the Physical Society, vol. 71, no. 4, p. 668, 1958.

[84] J. Wojewoda, A. Stefański, M. Wiercigroch, and T. Kapitaniak, "Hysteretic effects of dry friction: modelling and experimental studies," Philosophical Transactions of the Royal Society of London A: Mathematical, Physical and Engineering Sciences, vol. 366, no. 1866, pp. 747–765, 2008.

[85] P. R. Dahl, "Solid Friction Damping of Mechanical Vibrations," AIAA Journal, vol. 14, no. 12, pp. 1675–1682, 1976.

[86] B. Armstrong-Hélouvry, P. Dupont, and C. C. D. Wit, "A survey of models, analysis tools and compensation methods for the control of machines with friction," Automatica, vol. 30, no. 7, pp. 1083 – 1138, 1994.

[87] P.-A. J.Bliman, "Mathematical study of the Dahl ' s friction model," European Journal of Mechanics. A/Solids, vol. 11(6), no. June, pp. 835–848, 1992.

[88] K. Johanastrom and C. Canudas-De-Wit, "Revisiting the lugre friction model," IEEE control Systems, vol. 28, no. 6, pp. 101–114, 2008.

[89] E. Berger, "Friction modeling for dynamic system simulation," Applied Mechanics Reviews, vol. 55, no. 6, p. 535, 2002.

[90] T. Piatkowski, "Dahl and LuGre dynamic friction models: The analysis of selected properties," Mechanism and Machine Theory, vol. 73, pp. 91–100, 2014.

[91] F. P. Vidal, N. W. John, A. E. Healey, and D. A. Gould, "Simulation of ultrasound guided needle puncture using patient specific data with 3D textures and volume haptics," Computer Animation and Virtual Worlds, vol. 19, no. 2, pp. 111–127, 2008.

[92] Ka Wei Ng, Jin Quan Goh, Soo Leong Foo, Poh Hua Ting and T. K. Lee, "Needle Insertion Forces Studies for Optimal Surgical Modeling," Ijbbb, vol. 3, no. 6, pp. 187–191, 2013.

[93] R. J. Bacon, "An epidural injection simulator," vol. 45, no. June 1989, pp. 235–236, 1990.

[94] D. Tran, K.-W. Hor, A. A. Kamani, V. A. Lessoway, and R. N. Rohling, "Instrumentation of the loss-of-resistance technique for epidural needle insertion," IEEE Transactions on Biomedical Engineering, vol. 56, no. 3, pp. 820–827, 2009.

[95] S. Shin, W. Park, H. Cho, S. Park, and L. Kim, "Needle Insertion Simulator with Haptic Feedback," Human-Computer Interaction: Interaction Techniques and Environments, Pt Ii, vol. 6762, pp. 119–124, 2011.

[96] T. Dang, T. M. Annaswamy, and M. A. Srinivasan, "Development and evaluation of an epidural injection simulator with force feedback for medical training," Studies in Health Technology and Informatics, pp. 97–102, 2001.

[97] L. Bibin, L. Anatole, M. Bonnet, A. Delbos, and C. Dillon, "SAILOR: a 3-D medical simulator of loco-regional anaesthesia based on desktop virtual reality and pseudo-haptic feedback," ACM Sysmposium on Virtual Reality Software and Technology (VRST), pp. 97–100, 2008.

[98] O. Grottke, A. Ntouba, S. Ullrich, W. Liao, E. Fried, A. Prescher, T. M. Deserno, T. Kuhlen, and R. Rossaint, "Virtual reality-based simulator for training in regional anaesthesia," British Journal of Anaesthesia, vol. 103, no. 4, pp. 594–600, 2009.

[99] N. Vaughan, V. N. Dubey, M. Y. Wee, and R. Isaacs, "A review of epidural simulators: Where are we today?," Medical engineering & physics, vol. 35, no. 9, pp. 1235–1250, 2013.

[100] X. He, Y. Chen, and L. Tang, "Haptic simulation of flexible needle insertion," 2007 IEEE International Conference on Robotics and Biomimetics, ROBIO, pp. 607–611, 2008.

[101] R. J. Roesthuis, Y. R. Van Veen, A. Jahya, and S. Misra, "Mechanics of needle-tissue interaction," in 2011 IEEE/RSJ international conference on intelligent robots and systems, pp. 2557–2563, IEEE, 2011.

[102] G. A. Gescheider, Psychophysics: the fundamentals. Psychology Press, 2013.

[103] V. Klymenko, S. M. Pizer, and R. E. Johnston, "Visual Psychophysics and Medical Imaging: Nonparametric Adaptive Method for Rapid Threshold Estimation in Sensitivity Experiments," IEEE Transactions on Medical Imaging, vol. 9, no. 4, pp. 353–365, 1990.

[104] B. Wu, R. L. Klatzky, D. Shelton, and G. D. Stetten, "Psychophysical evaluation of in-situ ultrasound visualization," IEEE Transactions on Visualization and Computer Graphics, vol. 11, no. 6, pp. 684–693, 2005.

[105] I. J. Hirsh and C. S. Watson, "Auditory psychophysics and perception.," Annual review of psychology, vol. 47, pp. 461–84, 1996.

[106] R. S. Bernstein and J. S. Gravel, "A method for determining hearing sensitivity in infants: The interweaving staircase procedure (isp)," Journal of the American Academy of Audiology, vol. 1, no. 3, pp. 138–145, 1990.

[107] J. Huber, "The psychophysics of taste: Perceptions of bitterness and sweetness in iced tea," NA-Advances in Consumer Research Volume 01, 1974.

[108] L. M. Bartoshuk, "The psychophysics of taste.," The American Journal of Clinical Nutrition, vol. 31, no. 6, pp. 1068–1077, 1978.

[109] B. Johnson, R. M. Khan, and N. Sobel, "Human Olfactory Psychophysics," The Senses: A Comprehensive Reference, vol. 4, pp. 823–857, 2010.

[110] R. Henkin, "Evaluation and treatment of human olfactory dysfunction," Otolaryngology, vol. 2, pp. 1–86, 1993.

[111] S. J. Biggs and M. A. Srinivasan, "Haptic interfaces," Handbook of virtual Environments, pp. 93–116, 2002.

[112] S. McKnight, N. Melder, A. L. Barrow, W. S. Harwin, and J. P. Wann, "Psychophysical Size Discrimination using Multi-fingered Haptic Interfaces," Proceedings of 4th International Conference Eurohaptics 2004, pp. 274–281, 2004.

[113] N. Forrest, S. Baillie, and H. Z. Tan, "Haptic stiffness identification by veterinarians and novices: a comparison," Proceedings - 3rd Joint EuroHaptics Conference and Symposium on Haptic Interfaces for Virtual Environment and Teleoperator Systems, World Haptics 2009, pp. 646–651, 2009.

[114] G. Donlin, J. Dosher, and B. Hannaford, "Psychophysics of Multifinger Touch and Haptic Interfaces," p. 713028, 2008.

[115] L. A. Baumgart, G. J. Gerling, and E. J. Bass, "Psychophysical detection of inclusions with the bare finger amidst softness differentials," 2010 IEEE Haptics Symposium, HAPTICS 2010, pp. 17–20, 2010.

[116] D. A. Lawrence, L. Y. Pao, A. M. Dougherty, Y. Pavlou, S. W. Brown, and S. A. Wallace, "Human perception of friction in haptic interfaces," in Proc. ASME Dynamic Systems and Control Division, pp. 287–294, 1998.

[117] A. K. Frederick and P. Nicolaas, Psychophysics: A Practical Introduction. Elsevier, 2010.

[118] I. Nisky, A. Pressman, C. M. Pugh, F. A. Mussa-Ivaldi, and A. Karniel, "Perception and action in simulated telesurgery," Lecture Notes in Computer Science (including subseries Lecture Notes in Artificial Intelligence and Lecture Notes in Bioinformatics), vol. 6191 LNCS, no. PART 1, pp. 213–218, 2010.

[119] I. Nisky, A. Pressman, C. M. Pugh, F. A. Mussa-Ivaldi, and A. Karniel, "Perception and action in teleoperated needle insertion," IEEE Transactions on Haptics, vol. 4, no. 3, pp. 155–166, 2011.

[120] G. Brelstaff, M. Agus, A. Giachetti, E. Gobbetti, G. Zanetti, A. Zorcolo, B. Picasso, and S. S. Franceschini, "Towards a psychophysical evaluation of a surgical simulator for bone-burring," Proceedings of the 2nd symposium on Appied perception in graphics and visualization - APGV '05, p. 139, 2005.

[121] O. Gerovich, P. Marayong, and A. M. Okamura, "The effect of visual and haptic feedback on computer-assisted needle insertion.," Computer aided surgery : official journal of the International Society for Computer Aided Surgery, vol. 9, no. 6, pp. 243–249, 2004.

[122] H. Z. Tan, M. a. Srinivasan, B. Eberman, and B. Cheng, "Human factors for the design of force-reflecting haptic interfaces," ASME Dynamic Systems and Control (DSC), vol. 55, no. 1, pp. 353–359, 1994.

[123] L. A. Jones, "Matching forces: constant errors and differential thresholds," Perception, vol. 18, no. 5, pp. 681–687, 1989.

[124] H. H. King, R. Donlin, and B. Hannaford, "Perceptual thresholds for single vs. multi-finger haptic interaction," 2010 IEEE Haptics Symposium, HAPTICS 2010, pp. 95–99, 2010.

[125] X.-D. Pang, H. Z. Tan, and N. I. Durlach, "Manual discrimination of force using active finger motion," Perception & psychophysics, vol. 49, no. 6, pp. 531–540, 1991.

[126] M. R. Prasad, S. Purswani, and M. Manivannan, "Force jnd for right index finger using contra lateral force matching paradigm," in ICoRD'13, pp. 365–375, Springer, 2013.

[127] T. L. Brooks, "Telerobotic response requirements," in Systems, Man and Cybernetics, 1990. Conference Proceedings., IEEE International Conference on, pp. 113–120, IEEE, 1990.

[128] L. Batteau, A. Liu, and J. Maintz, "A study on the perception of haptics in surgical simulation," Medical Simulation, vol. 3078, pp. 185–192, 2004.

[129] M. H. Zadeh, D. Wang, and E. Kubica, "Human Factors for Designing a Haptic Interface for Interaction with a Virtual Environments," IEEE International Workshop on Haptic Audio Visual Environments and their Applications, no. October, pp. 12–14, 2007.

[130] L. A. Jones and H. Z. Tan, "Application of psychophysical techniques to haptic research," IEEE Transactions on Haptics, vol. 6, no. 3, pp. 268–284, 2013.

Gourishetti Ravali received the BTech degree in electronics and instrumentation from Kakatiya University, Warangal and the MTech degree in biomedical engineering from MNNIT Allahabad, Allahabad in 2012 and 2014 respectively. She joined Haptics Lab, IIT Madras, as a research scholar in 2014.

Muniyandi Manivannan received the ME and PhD degrees from the Indian Institute of Science, Bangalore. He received post-doctoral training in Haptics at MIT, Cambridge. Before MIT, he received another post-doctoral training in CAD standards and sensors network at the National Institute of Standards and Technology, Maryland. He served as a chief software architect of Yantric Inc. before joining IIT Madras.